

Supplementary Material

From water into sediment - tracing freshwater cyanobacteria via DNA analyses

Ebuka Canisius Nwosu*, Patricia Roeser, Sizhong Yang, Lars Ganzert, Olaf Dellwig, Sylvia

Pinkerneil, Achim Brauer, Elke Dittmann, Dirk Wagner and Susanne Liebner

* Correspondence:

enwosu@gfz-potsdam.de

This file includes;

Supplementary information: Extended Materials and Methods

Supplementary Figures

Figure S1: Distribution of all cyanobacteria ASVs among sample types of Lake Tiefer See.

Figure S2: Variation of environmental variables from water and sediment traps of Lake Tiefer See.

Figure S3: Cyanobacteria distribution and abundance in Lake Tiefer See.

Figure S4: Rank-based Spearman correlation

Figure S5: Heatmaps of relative abundances of all amplicon sequence variants (ASVs) assigned to a) Aphanizomenon, b) Microcystis, and c) Snowella.

Figure S6: Chlorophyll-a and dissolved oxygen for the month of August 2019 throughout the water column of Lake Tiefer See.

Supplementary Tables

Table S1: Statistical analyses of sequencing analysis and alpha diversity data.

Table S2: Rank-based Spearman correlation coefficients.

Table S3: Similarity percentage (SIMPER) test on the cyanobacteria ASVs.

Table S4: Total sulfide measurements from water column samples.

Table S5: Nitrate measurements from water column samples.

Table S7: Significant explanatory parameters used in the Spearman correlation analysis

Supplementary Information: Extended Materials and Methods

Study site. The hard water oligo-mesotrophic Lake Tiefer See (near Klocksín; 53°35.5'N, 12°31.8'E; 62 m a.s.l.) is part of the southern Baltic Lake District and was formed during the final stage of the last glacial period (~13,000 years ago) (Dräger et al., 2017; Fig. 1a, b). Lake Tiefer See is part of a subglacial gully system in a morainic terrain located in Nature Park 'Nossentiner/Schwinzer Heide.' Today, the lake is connected to Lake Hofsee in the south through a shallow sill, whereas the connection to Lake Flacher See in the north has been channelized into a tunnel after the construction of a railway dam between the two lakes (CE 1884–1886) and is currently largely interrupted. Lake Tiefer See has a surface area of approximately 0.75 km², and the catchment area of approximately 5.5 km² is dominated by glacial till. Although the catchment is mainly used for agriculture (Theuerkauf et al. 2015), the direct shore-line of the lake is covered by a fringe of trees, and there is no anthropogenic infrastructure, such as buildings or roads at the lakeshore. The lake has a maximum depth of 62 m and no major inflows or outflow. The annual lake mixing is either mono- or dimictic, depending on the formation of a winter ice cover (Kienel et al. 2017). The study site is characterized by a warm-temperate climate during the transition from oceanic to continental conditions. Mean monthly temperatures range from 0°C in January to 17–18°C in July, with maxima up to 30°C and minima down to -5°C. Mean monthly precipitation varies between ~40 mm during winter and ~60 mm in summer, with a mean annual precipitation of 560–570 mm (Kienel et al. 2017). Lake Tiefer See has been the focus of an extensive and high-resolution climate monitoring program since the beginning of the last decade (Roeser et al. 2021). The lake is well-preserved and seasonally laminated sediments have aided climate reconstructions spanning the last 6,000 years (e.g., Dräger et al. 2019).

Collection of water, sediment trap material, and sediment cores

Water samples were collected monthly between January 30 and November 28, 2019, at the floating weather monitoring station, located at the maximum depth of the lake (62 m; Fig. 1b). The sampled water depths were 1, 3, 5, 7, 10, 15, 20, 40, 45, and 50 m. A sample volume of 250 mL of lake water was collected for the upper 1, 3, and 5 m water depths and pooled (750 mL), representing the epilimnion. Likewise, 375 mL volumes were collected for the lower 45 and 50 m water depths and pooled (750 mL), representing the bottom waters. For each of the other 7, 10, 15, 20, and 40 m water depths, 750-mL water samples were collected. The samples were collected in sterile glass bottles (Schott Duran®, Germany), filtered within 24 h after fieldwork using 0.2 µm cellulose filters (Sartorius AG, Germany), and the filters were stored at -20°C until nucleic acid extraction.

The suspended particulate matter was trapped with four-cylinder traps (KC Denmark A/S total active area 0.0163 m² for the four cylinders) at two depths in the water column (Fig. 1c). One trap was anchored in the metalimnion (12 m water depth), whereas the second trap was secured in the hypolimnion (55 m water depth). For both depths, the traps were emptied monthly between April and November 2019, i.e., the annual interval of increased lake productivity. The trapped material was transferred into 2 L plastic bottles, which were allowed to settle overnight at 4°C. An equal volume of water was discarded from the bottles, and the remaining suspension was transferred into sterile 50 mL Falcon tubes (Fischer Scientific GmbH, Germany). The tubes containing suspended particulate matter were then centrifuged at 4000 g for 5 min. Subsequently, the supernatant was discarded, and the pellet was stored in Falcon tubes at -20°C until nucleic acid extraction.

A surface sediment core (TSK19-SC6; 115 cm length) was collected on August 29, 2019, from the point of maximum water depth (62 m) using a 90 mm UWITEC piston corer. The temperature of the upright positioned core was maintained at 4 °C during transportation and short-term storage at the facilities of the GFZ Potsdam. To preserve the uppermost varves, the core was allowed to dry in a vertical position at 4 °C for approximately 2 weeks before longitudinal splitting. After splitting the core, one half was lithologically described. A triplicate 0–2 cm subsample of the other core half was stored in sterile 15 mL Falcon tubes at -20°C until nucleic acid extraction. All core handling was performed under clean

conditions in a room where no molecular biological work had been previously conducted to avoid contamination.

Lake physicochemical properties

Measurements of the physicochemical parameters, such as temperature, pH, dissolved oxygen (DO), turbidity, and chlorophyll-a (Chla) in the water column were conducted automatically using a multi-parameter water quality probe (YSI 6600 V2, Yellow Springs USA), in 1-m steps and 12 h resolution. Owing to technical problems, in February, data were only collected on 2 d (1st and 28th), and in March, no data were recorded between the 2nd and 10th. Water temperature was additionally measured using 26 stationary data loggers (HOBO Water Temp Pro v2, Onset USA) in 1-m steps from 0 to 15 m and 5-m steps from 15 to 55 m water depth (Fig. 1c). Water samples for nitrate (NO_3^-) and total dissolved phosphorus (TDP) analyses were also collected monthly, in parallel with those for molecular analysis. Water samples for total sulfide were collected from the hypolimnion in October and November. Water samples for nitrate measurements were analyzed at the German Research Centre for Geosciences (GFZ), whereas TDP and total sulfide were conducted at the Leibniz Institute for Baltic Sea Research Warnemünde (IOW). Nitrate was measured by suppressed ion chromatography using a SeQuant SAMS anion IC suppressor (EMD Millipore, Billerica, Massachusetts), an S5200 sample injector, a 3.0×250 mm LCA 14 column, and an S3115 conductivity detector (all Sykam, Fürstfeldbruck, Germany). The eluent was 5 mM Na_2CO_3 , 20 mg L^{-1} 4-hydroxybenzonitrile and 0.2% methanol. The flow rate was set to 1 mL min^{-1} , and the column oven temperature was to 50°C . The detection and quantification limits were calculated based on signal-to-noise (S/N) ratios of 3 and 10, respectively. All samples were measured in triplicate, and every 10 injections a standard was measured to check for drift. Reproducibility was always better than 5%, and the detection limit ranged between 1–4 μM . For TDP, the water samples were immediately filtered using 0.45 μm syringe filters and acidified with sub-boiled HNO_3 to 2 vol%. The TDP was measured by inductively coupled plasma optical emission spectrometry (ICP-OES; iCAP 7400, Duo, Thermo Fisher Scientific) using external calibration and Sc as the internal

standard. Precision and trueness were checked with the international reference material SLRS-6 (NRCC) spiked with 20 µg L⁻¹ P, which were 9.6% and 5.7%, respectively. After fixation of 50 mL of an aliquot of the filtered water sample with 500 µL 20 vol% zinc acetate solution, total sulfide was determined spectrophotometrically according to the Cline method (Cline, 1969) with a precision of 3.2% (Dellwig et al. 2019).

The sediment fluxes (sediment flux: g m⁻² d⁻¹) were determined from the weighted and freeze-dried trapped sediment material. The samples were homogenized using an agate mortar. Prior to total organic carbon (TOC) and total nitrogen (TN) determination, replicate aliquots (0.2 mg) were decalcified in situ in Ag capsules (20% HCl and dried at 75°C). The TOC and TN contents were measured using the elemental analyzers NC2500 and EA3000-CHS Eurovectors, respectively, and were used to calculate the atomic C:N ratio. CaCO₃ content was estimated after obtaining the total inorganic carbon content (TIC = TC–TOC) and multiplying by a factor of 8.33, which is the percentage of molecular weight in inorganic carbon in the calcium carbonate structure.

Molecular analyses

All nucleic acid extractions were conducted in a clean laboratory where no polymerase chain reaction (PCR) was performed prior to the extraction, following established methods and precautions to limit contamination. Water sample DNA extraction was performed at different times than the sediment samples to avoid cross-contamination. Additionally, the sediment traps were processed independently from the surface sediment cores. Because of water column turnover in January and February, water samples for molecular analyses from 1, 3, 5, 7, and 10 m water depths were pooled and reported as the mean depth (5 m). Water depths of 40, 45, and 50 m were equally pooled and reported as the mean depth (45 m). In March, when temperatures began to increase, four depths in the water column were reported as follows: 5 (1, 3, 5, and 7 m pooled), 10, 20, and 45 m (40, 45, and 50 m pooled). Genomic DNA (gDNA) of water samples was extracted from the filters using the DNeasy PowerWater Kit (QIAGEN, Hilden, Germany) following the manufacturer's specifications. The gDNA from the

homogenized sediment trap samples and surface sediment samples was extracted from approximately 0.75 g using the DNeasy PowerSoil Kit (QIAGEN, Hilden, Germany). The extracted gDNA from all samples was eluted in 100 µL elution buffer and stored at -20°C until downstream analysis.

Cyanobacteria quantification Total cyanobacteria were quantified with a SYBR Green qPCR assay that specifically amplified the cyanobacterial 16S rRNA-ITS (internal transcribed spacer) region using the primers CSIF (5'-GYCACGCCCCGAAGTCRTTAC-3') and 373R (5'-CTAACCACCTGAGCTAAT-3') (Janse et al., 2003). The final volume of the qPCR reactions was 20 µL, which consisted 10 µL of KAPA HiFi 2x SensiFAST SYBR® FAST qPCR Master Mix (Sigma-Aldrich, Germany), 0.2 µL of each forward and reverse primer (100 µM, Biomers), 5.8 µL PCR water, and 4 µL of template DNA. The qPCR program consisted of an initial polymerase activation step (95°C for 15 min), followed by 40 cycles of denaturation at 94°C for 60 s, annealing at 60°C for 60 s, and extension at 72°C for 60 s. The qPCR program was followed by a melting curve step from 70°C to 95°C at a transition rate of 1°C per 5 s to determine the specificity of the amplification. The amplified products were confirmed using agarose gel electrophoresis. Tenfold dilution standards were prepared from gDNA of *Synechocystis* for each qPCR assay, which ranged from 4.7×10^7 to 4.7×10^3 copies ng⁻¹ DNA, and was used to create the standard curves from which the quantification cycle (C_q) values were determined (Bustin et al. 2009). The copy numbers of the 16S rRNA-ITS region were calculated following Savichtcheva et al. (2011), and were the mean of triplicates of each sample expressed as cyanobacterial abundance normalized to extracted DNA (copies ng⁻¹ DNA) with a minimum quantification efficiency of 91%. All qPCR assays were performed in triplicate on a CFX96 real-time thermal cycler (Bio-Rad Laboratories, Inc., USA).

Sequence library preparation All consumables and pipets used for PCR were sterilized in a laminar flow hood under UVC light for at least 15 min prior to use. PCR for the Illumina high-throughput sequencing (HTS) libraries was conducted using the cyanobacteria-specific primers CYA359F (5'-CGGACGGGTGAGTAACGCGTG-3') and CYA784R (5'-ACTACWGGGGTATCTAATCCC-3') (Nübel et al. 1997). They amplify a >400-nt-long fragment of the V3–V4 regions of the 16S rRNA gene. The

primers had unique tags (Supplemental Information SI 1) that served to differentiate the samples. The water and sediment samples, as well as the negative control (that is, a reaction with PCR water as a template) were amplified in a PCR reaction of 50 μ L, containing 10x Pol Buffer C (Roboklon GmbH, Berlin, Germany), 25 mM MgCl₂, 0.2 mM deoxynucleoside triphosphate (dNTP) mix (ThermoFisher Scientific), 0.5 mM each primer (TIB Molbiol, Berlin, Germany) and 1.25 U of Optitaq Polymerase (Roboklon). The volume of the template DNA used in each reaction varied between 1 and 4 μ L, depending on the sedDNA concentration. The PCR program included an initial denaturation step at 95°C for 10 min, followed by 35 cycles at 95°C for 15 s, annealing at 60°C for 30 s, extension at 72°C for 45 s, and a final extension step at 72°C for 5 min. To avoid cross-contamination, the PCR reactions were performed monthly after each sampling, and the water samples were processed separately from the sediment samples. The tagged PCR products were then purified with the Agencourt AMPure XP kit (Beckman Coulter, Brea, CA, USA) and eluted in 30 μ L DNA/RNA-free water. The purified product was quantified using a Qubit (2.0) fluorometer. Equimolar concentrations of all samples, including two negative purified PCR controls, were pooled into two multiplex libraries (n = 160 samples, including 78 samples and 2 controls per library). The two libraries contained technical replicates of the water samples and biological replicates of the sediment samples. The final libraries were paired-end sequenced (2 × 300 bp) on an Illumina MiSeq system (Eurofins Scientific (Constance, Germany)).

Bioinformatics. The obtained 14,649,824 sequence reads were quality checked on a raw FASTQ file with FastQC (Andrews et al. 2015). The reads were then demultiplexed using the make.contigs function in Mothur (v.1.39.5: pdiff=2, bdiff=1, and default settings for others) (Schloss et al. 2009). Based on the report files, the sequence identifiers were retrieved for those sequences with minimum overlap (length > 25), maximum mismatches (< 5), and the maximum number of ambiguous bases of zero (which means there was no base marked with N'). According to the sequence identifiers from the previous step, the sequences were then extracted with the filterbyname.sh function from BBtools (Bushnell et al. 2017)

from the raw paired-end fastq files. This step was followed by checking and correcting the sequence orientation and removing sample unique barcodes using `extract_barcodes.py` in QIIME1 (Caporaso et al., 2010). Finally, primers were removed using Cutadapt (Martin 2014). The sequences were then fed to DADA2 (Callahan et al. 2016) for filtering, dereplication, chimera check, sequence merge, and amplicon sequence variant (ASV) calling. Then, QIIME2 (Bolyen et al. 2019) was used for taxonomic assignment against the SILVA138 database (Quast et al. 2013).

Data availability. Sequencing data and metadata are deposited in the European Nucleotide Archive (ENA) under BioProject accession number PRJEB40406 and sample accession numbers ERS5083533-ERS5083564 (trap material and surface sediment samples) and ERS5083566-ERS5083644 (water samples).

Sequence data processing. The 152 samples resulted in a total of 7,297,946 denoised and error-corrected sequences that DADA2 inferred in 2,538 ASVs. We filtered out all ASVs not assigned to cyanobacteria and chloroplasts, and another 43 ASVs that occurred in fewer than three samples over the entire dataset to reduce bias from very rare taxa. The four negative controls that were included in the sequencing run each comprised less than 1% of the reads compared with the sample average and were therefore removed.

References of the extended materials and methods

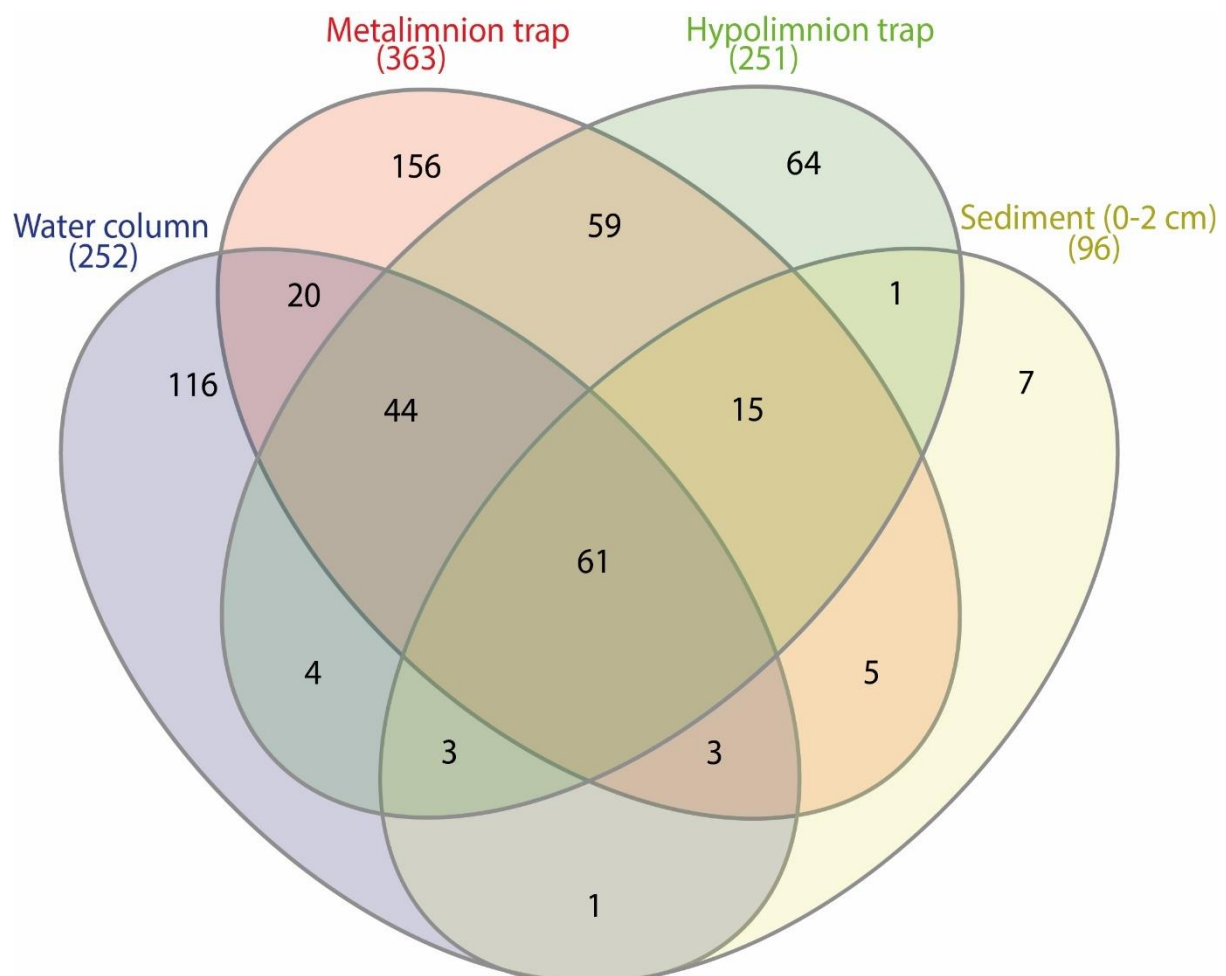
- Andrews, S., F. Krueger, A. Seckerson-Pichon, F. Biggins, and S. Wingett. 2015. FastQC. A quality control tool for high-throughput sequence data. Babraham Bioinformatics. Babraham Inst.
- Bushnell, B., J. Rood, and E. Singer. 2017. BBTools software package. PLOS ONE **12**: e0185056, doi:[10.1371/journal.pone.0185056](https://doi.org/10.1371/journal.pone.0185056)
- Bustin, S. A., and others 2009. The MIQE guidelines: Minimum information for publication of quantitative real-time PCR experiments. Clin. Chem. **55**: 611-622. doi:[10.1373/clinchem.2008.112797](https://doi.org/10.1373/clinchem.2008.112797)

- Callahan, B. J., P. J. McMurdie, M. J. Rosen, A. W. Han, A. J. A. Johnson, and S. P. Holmes. 2016. DADA2: High-resolution sample inference from Illumina amplicon data. *Nat. Methods*. **13**: 581-583. doi:[10.1038/nmeth.3869](https://doi.org/10.1038/nmeth.3869)
- Caporaso, J. G., and others. 2010. QIIME allows analysis of high-throughput community sequencing data. *Nat. Methods*. **7**: 335-336. doi:[10.1038/nmeth.f.303](https://doi.org/10.1038/nmeth.f.303)
- Cline, J. D. 1969. Spectrophotometric determination of hydrogen sulfide in natural waters. *Limnol. Oceanogr.* **14**: 454-458. doi:[10.4319/lo.1969.14.3.0454](https://doi.org/10.4319/lo.1969.14.3.0454)
- Czymzik, M., R. Muscheler, F. Adolphi, and others. 2018. Synchronizing ¹⁰Be in two varved lake sediment records to IntCal13 ¹⁴C during three grand solar minima. *Clim. Past*. **14**: 687-696. doi:[10.5194/cp-14-687-2018](https://doi.org/10.5194/cp-14-687-2018)
- Dellwig, O., A. Wegwerth, B. Schnetger, H. Schulz, and H. W. Arz. 2019. Dissimilar behaviors of the geochemical twins W and Mo in hypoxic-euxinic marine basins. *Earth Sci. Rev.* **193**: 1-23. doi:[10.1016/j.earscirev.2019.03.017](https://doi.org/10.1016/j.earscirev.2019.03.017)
- Dräger, N., B. Plessen, U. Kienel, M. Słowiński, A. Ramisch, R. Tjallingii, S. Pinkerneil, and A. Brauer. 2019. Hypolimnetic oxygen conditions influence varve preservation and $\delta^{13}\text{C}$ of sediment organic matter in Lake Tiefer See, NE Germany. *J. Paleolimnol.* **62**: 181-194. doi:[10.1007/s10933-019-00084-2](https://doi.org/10.1007/s10933-019-00084-2)
- Dräger, N., M. Theuerkauf, K. Szeroczyńska, S. Wulf, R. Tjallingii, B. Plessen, U. Kienel, and A. Brauer. 2017. Varve microfacies and varve preservation record of climate change and human impact for the last 6000 years at Lake Tiefer See (NE Germany). *Holocene* **27**: 450-464. doi:[10.1177/0959683616660173](https://doi.org/10.1177/0959683616660173)
- Janse, I., M. Meima, W. E. A. Kardinaal, and G. Zwart. 2003. High-resolution differentiation of cyanobacteria by using rRNA-internal transcribed spacer denaturing gradient gel electrophoresis. *Appl. Environ. Microbiol.* **69**: 6634-6643. doi:[10.1128/AEM.69.11.6634-6643.2003](https://doi.org/10.1128/AEM.69.11.6634-6643.2003)
- Kienel, U., G. Kirillin, B. Brademann, B. Plessen, R. Lampe, and A. Brauer. 2017. Effects of spring warming and mixing duration on diatom deposition in deep Tiefer See, NE Germany. *J. Paleolimnol.* **57**: 37-49. doi:[10.1007/s10933-016-9925-z](https://doi.org/10.1007/s10933-016-9925-z)
- Martin, M. 2014. Cutadapt removes adapter sequences from high-throughput sequencing reads. *EMBnet. J.* **17**: 10-12. doi:[10.14806/ej.17.1.200](https://doi.org/10.14806/ej.17.1.200)
- Nübel, U., F. Garcia-Pichel, and G. Muyzer. 1997. PCR primers to amplify 16S rRNA genes from cyanobacteria. *Appl. Environ. Microbiol.* **63**: 3327-3332
- Quast, C., E. Pruesse, P. Yilmaz, J. Gerken, T. Schweer, P. Yarza, J. Peplies, and F. O. Glöckner. 2013. The SILVA ribosomal RNA gene database project: Improved data processing and web-based tools. *Nucleic Acids Res.* **41**: D590-D596. doi:[10.1093/nar/gks1219](https://doi.org/10.1093/nar/gks1219)
- Roeser, P., N. Dräger, D. Brykała, and others. 2021. Advances in understanding calcite varve formation: New insights from a dual lake monitoring approach in the southern Baltic lowlands. *Boreas* **50**: 419-440. doi:[10.1111/bor.12506](https://doi.org/10.1111/bor.12506)
- Savichtcheva, O., D. Debroas, R. Kurmayer, C. Villar, J. P. Jenny, F. Arnaud, M. E. Perga, and I. Domaizon. 2011. Quantitative PCR enumeration of total/toxic *Planktothrix rubescens* and total cyanobacteria in preserved DNA isolated from lake sediments. *Appl. Environ. Microbiol.* **77**: 8744-8753. doi:[10.1128/AEM.06106-11](https://doi.org/10.1128/AEM.06106-11)

- Savichtcheva, O., D. Debroas, M. E. Perga, and others. 2015. Effects of nutrients and warming on *Planktothrix* dynamics and diversity: A palaeolimnological view based on sedimentary DNA and RNA. *Freshw. Biol.* **60**: 31-49. doi:[10.1111/fwb.12465](https://doi.org/10.1111/fwb.12465)
- Schloss, P. D., and others. 2009. Introducing Mothur: Open-source, platform-independent, community-supported software for describing and comparing microbial communities. *Appl. Environ. Microbiol.* **75**: 7537-7541. doi:[10.1128/AEM.01541-09](https://doi.org/10.1128/AEM.01541-09)
- Theuerkauf, M., N. Dräger, U. Kienel, A. Kuparinen, and A. Brauer. 2015. Effects of changes in land management practices on pollen productivity of open vegetation during the last century derived from varved lake sediments. *Holocene.* **25**: 733-744. doi:[10.1177/0959683614567881](https://doi.org/10.1177/0959683614567881)

Supplementary Figures

Figure S1. Distribution of all cyanobacteria ASVs among sample types of Lake Tiefer See



Venn diagram shows distribution of the 559 cyanobacterial amplicon sequence variants (ASVs) among the sample types.

Figure S2. Variation of environmental variables from water and sediment traps of Lake Tiefer See: Principal components analyses (PCA) of environmental data based on Euclidean distance from (a) water column with percentage variation between samples from the thermal stratification zones indicated on the principal components PC1 and PC2 axes. Total variance explained by both axes = 64.14%. Epilimnion n = 19, metalimnion n = 16 and hypolimnion n = 12. (b) meta- (orange; n = 8) and hypolimnion (cyan; n = 8) sediment trap samples. Both PC1 and PC2 together explain 76.61% of total variance among the samples. In both plots the environmental variables are projected as green vectors.

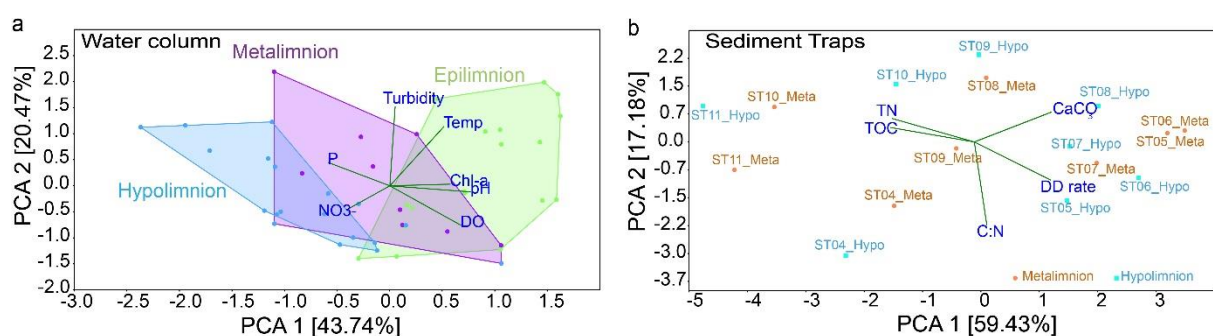


Figure S3. Cyanobacteria community distribution in Lake Tiefer See (a) Bubble plot showing spatial (depth) and temporal (monthly) variation of the most abundant cyanobacteria ASVs (> 1% reads) in 2019, and (b) Cyanobacterial abundance quantified via qPCR with primers that

amplify part of the 16S rRNA internal transcriber spacer (ITS) region of cyanobacteria (data were normalized to ng DNA extracted). Blue vertical lines represent the average abundance in each depth while broken blue vertical line represents overall averages in water column and sediment traps, respectively.

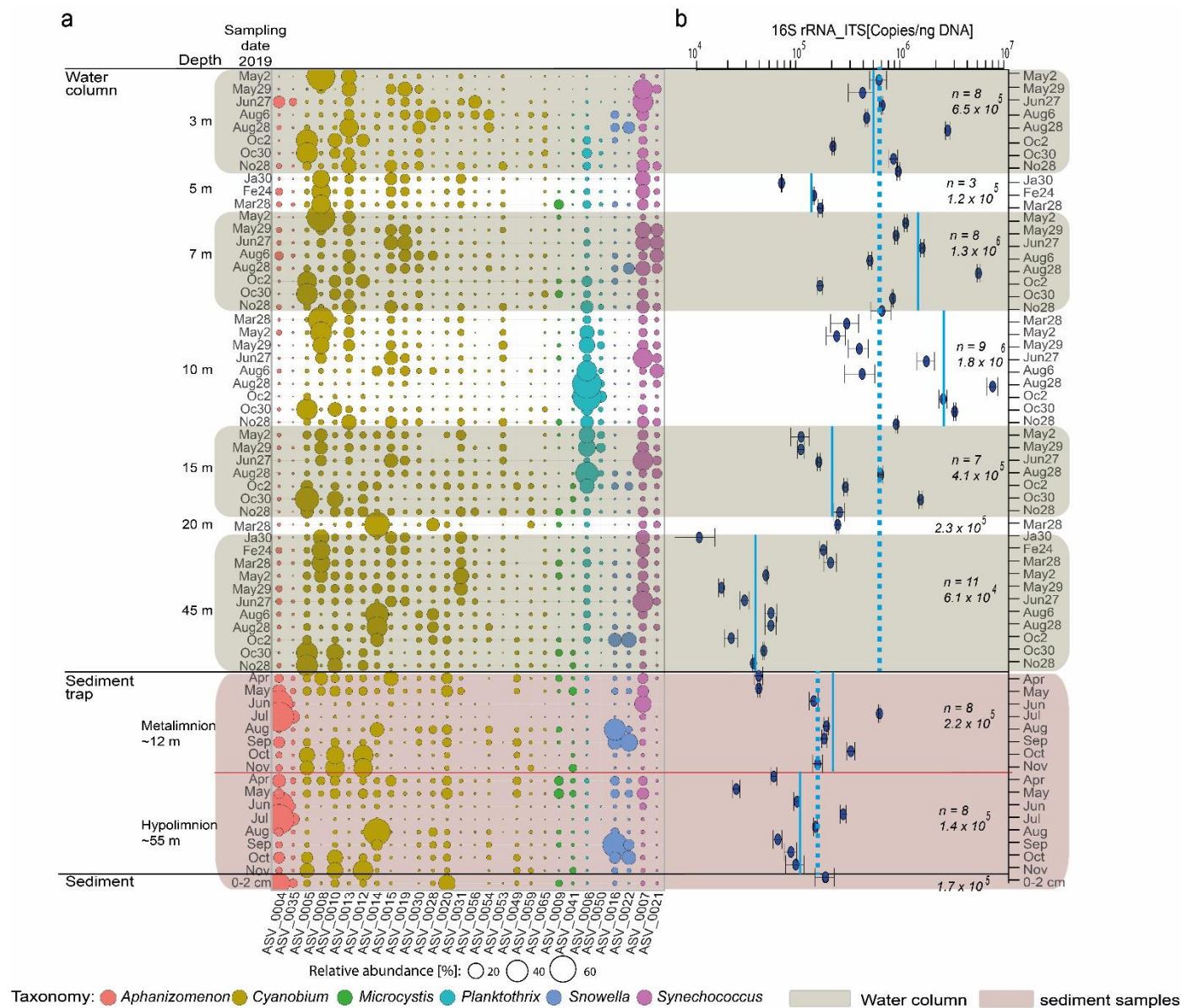


Figure S4 Rank based spearman correlation of the total cyanobacteria community composition from the hypolimnion trap with internal physicochemical parameters in Lake Tiefer See. Blue bubbles show positive while red bubbles show negative correlation. The p values are shown below the figure.

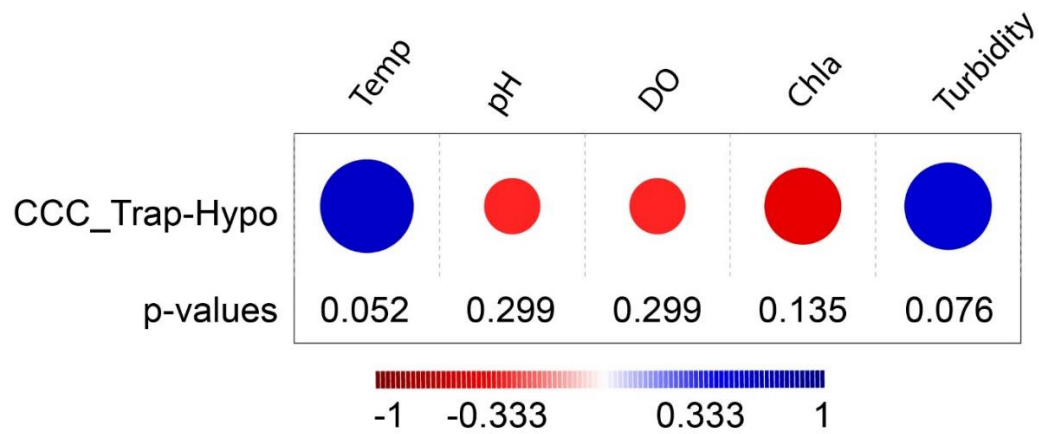


Figure S5 Heatmaps of relative abundances of all amplicon sequence variants (ASVs) assigned to (a) *Aphanizomenon*, (b) *Microcystis*, and (c) *Snowella*. Data is interpolated for 15 days and 5 m water depth. Black circles and red squares represent the depths and timing of sampling of water and sediment traps, respectively.

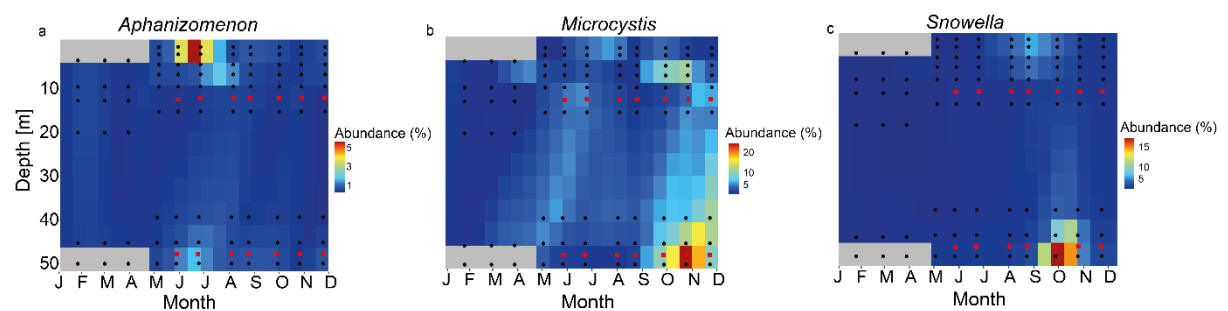
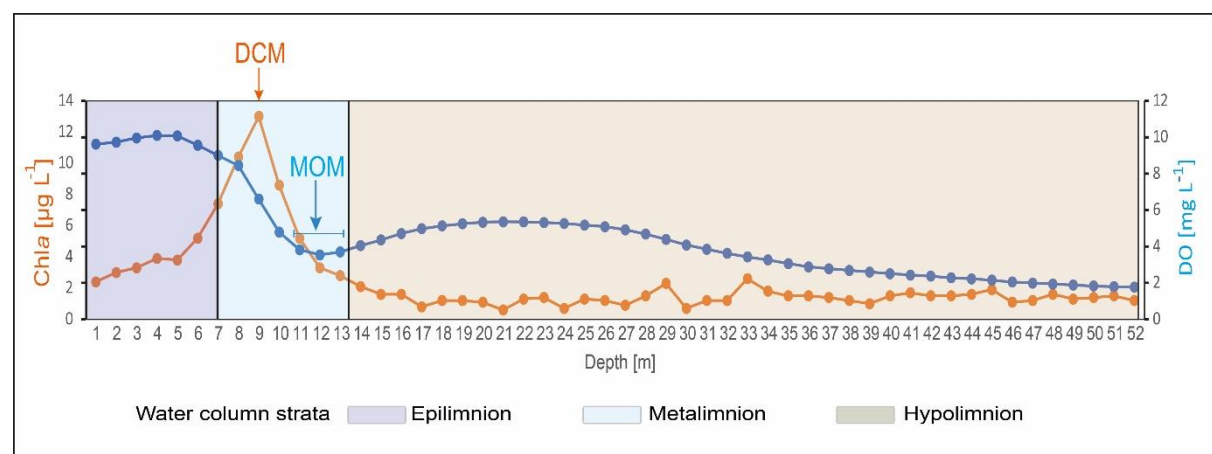


Figure S6. Chlorophyll a and dissolved oxygen for the month of August 2019 throughout the water column of Lake Tiefer See showing the formation of deep chlorophyll maximum (DCM) and the metalimnetic oxygen minimum (MOM) layers in the metalimnion.



Supplementary Tables

Table S1. Statistical analyses of sequencing analysis and alpha diversity data.

Sample Site	Sample ID	Raw read counts	Quality filtered read counts	Cyanobacteria read counts	Observed ASVs >1%	Shannon_H >1%	Pielou's Evenness >1%	Barcode sequence-F	Barcode sequence-R
Epilimnion water column	May2_3	175384	98630	81793	25	1,055	0,1149	CATCCAGT	CGTGATAC
	May29_3	222133	92445	72541	23	1,872	0,2827	CATCCAGT	CTTCTTCC
	Jun_3	149317	48309	45708	25	2,179	0,3534	CATCCAGT	TATCCTCC
	Aug6_3	150922	45764	42420	26	2,648	0,5435	CATCCAGT	AACACCGT
	Aug28_3	91961	31111	28751	26	2,378	0,4149	CATCCAGT	TTACCGCT
	Oc2_3	281533	114661	94889	26	2	0,2841	CATCCAGT	TGAGATGC
	Oc30_3	62337	26642	24724	27	2,139	0,3146	CATCCAGT	GTGCAACT
	No_3	143307	43009	33877	27	2,619	0,5081	CATCCAGT	TGAGCCTA
	Ja5	165673	84153	26826	27	2,307	0,3722	CAACCTCA	CGTGATAC
	Fe5	141976	66220	9396	25	2,38	0,4322	CAACCTCA	CTTCTTCC
	Mar_5	188223	116484	6880	25	2,594	0,5353	CAACCTCA	TATCCTCC
	May2_7	143438	76718	53025	26	1,21	0,1289	CAACCTCA	AACACCGT
	May29_7	87050	32700	19614	26	2,5	0,4684	CAACCTCA	TTACCGCT
	Jun_7	121635	45534	28964	26	2,284	0,3776	CAACCTCA	TGAGATGC
	Aug6_7	113860	41923	29158	27	2,694	0,5476	CAACCTCA	GTGCAACT
	Aug28_7	125613	38114	27369	27	2,685	0,5431	CAACCTCA	TGAGCCTA
Metalimnion water column	Oc2_7	165231	74945	42161	27	2,288	0,3652	CAACCTCA	ATGGAGGT
	Oc30_7	110619	44863	33462	27	2,169	0,3242	CAACCTCA	CTGAGTCT
	No_7	98597	30472	19070	26	2,605	0,5206	CAACCTCA	GAGGTGAA
	Mar_10	179609	90856	16944	25	1,761	0,2326	TGCTTGTC	CGTGATAC
	May2_10	130479	63282	12305	24	2,101	0,3405	TGCTTGTC	CTTCTTCC
	May29_10	156049	63943	38722	25	2,231	0,3723	TGCTTGTC	TATCCTCC
	Jun_10	142750	63870	32767	26	2,236	0,3598	TGCTTGTC	AACACCGT
	Aug6_10	123174	47865	32423	27	2,308	0,3723	TGCTTGTC	TTACCGCT
	Aug28_10	137861	66836	50276	26	1,21	0,129	TGCTTGTC	TGAGATGC
	Oc2_10	120789	70191	60084	27	1,149	0,1169	TGCTTGTC	GTGCAACT
	Oc30_10	133799	49913	37460	27	2,126	0,3105	TGCTTGTC	TGAGCCTA
	No_10	142473	51925	30701	27	2,597	0,497	TGCTTGTC	ATGGAGGT
	May2_15	81787	46493	2269	20	2,568	0,652	TCGTCGCTCG	CTTCTTCC
	May29_15	80368	40667	4737	22	2,47	0,5374	TCGTCGCTCG	TATCCTCC
	Jun_15	41918	18060	16238	24	2,209	0,3795	TCGTCGCTCG	AACACCGT
	Aug28_15	42116	18868	17440	27	2,311	0,3735	TCGTCGCTCG	TGAGATGC
Hypolimnion Water column	Oc2_15	51271	20196	11927	27	2,852	0,6417	TCGTCGCTCG	GTGCAACT
	Oc30_15	50931	24740	21906	27	1,738	0,2105	TCGTCGCTCG	TGAGCCTA
	No_15	48673	22522	14514	27	2,884	0,6626	TCGTCGCTCG	ATGGAGGT
	Mar_20	95758	46951	6179	22	2,047	0,352	TCGTCGCTCG	CGTGATAC
	Ja45	171550	91611	34366	26	2,457	0,4487	AGACGCACTC	CGTGATAC
	Fe45	114796	48626	9228	25	2,476	0,4756	AGACGCACTC	CTTCTTCC
	Mar_45	221091	101049	10111	26	2,639	0,5384	AGACGCACTC	TATCCTCC
	May2_45	153557	88720	13370	27	2,708	0,5553	AGACGCACTC	AACACCGT
	May29_45	156154	95642	15194	27	2,841	0,6345	AGACGCACTC	TTACCGCT
	Jun_45	177970	45534	37373	27	2,426	0,4188	AGACGCACTC	TGAGATGC
	Aug6_45	80692	36232	19745	27	2,084	0,2975	AGACGCACTC	GTGCAACT
	Aug28_45	129908	52656	39619	27	2,439	0,4245	AGACGCACTC	TGAGCCTA
	Oc2_45	202697	110256	56113	27	2,625	0,5114	AGACGCACTC	ATGGAGGT
	Oc30_45	109925	58519	42235	27	1,985	0,2696	AGACGCACTC	CTGAGTCT
	No_45	116083	58165	29652	27	2,126	0,3103	AGACGCACTC	GAGGTGAA
Metalimnion Sediment Trap	ST04M	148116	96606	25447	24	2,669	0,6011	GGTAGTTCT	CTGAGTCT
	ST05M	103171	76608	6266	21	2,754	0,7477	GGTAGTTCT	GAGGTGAA
	ST06M	103612	62935	36315	21	1,095	0,1423	GGTAGTTCT	GGCATGTA
	ST07M	71344	54145	52049	24	0,9098	0,1035	CGTAAGTC	CTGAGTCT
	ST08M	87695	41455	22985	25	2,15	0,3435	CGTAAGTC	GAGGTGAA
	ST09M	121584	65137	52867	26	2,444	0,443	CGTAAGTC	GGCATGTA
	ST10M	83235	39122	29311	22	1,779	0,2692	AACTGTCC	GAGGTGAA
Hypolimnion Sediment Trap	ST11M	394735	157394	107948	26	1,768	0,2253	AACTGTCC	GGCATGTA
	ST04H	131181	104465	8796	25	2,868	0,704	TCACGTACTA	GAGGTGAA
	ST05H	117673	85782	16330	25	2,871	0,706	TCACGTACTA	GGCATGTA
	ST06H	70692	47525	26943	26	1,062	0,1112	CGCATAGA	GTGCAACT
	ST07H	141180	101235	76740	27	0,8603	0,08755	CGCATAGA	TGAGCCTA
	ST08H	62645	35007	25681	25	1,648	0,2079	CGCATAGA	ATGGAGGT
	ST09H	116154	63122	46134	25	1,87	0,2595	CGCATAGA	CTGAGTCT
Sed	ST10H	77117	32037	29331	24	2,429	0,4727	CGCATAGA	GAGGTGAA
	ST11H	115038	49838	22808	21	1,996	0,3503	CGCATAGA	GGCATGTA
Sed	Sed	65357	35215	10585	23	2,046	0,3365	TCCTGGTA	GTGCAACT

Table S2. Rank-based Spearman correlation coefficients of the most abundant cyanobacteria ASVs, total cyanobacteria community composition, cyanobacteria 16S rRNA-ITS gene abundance with internal physicochemical parameters in Lake Tiefer See. Values in bold are significant at $p < 0.05$ with Bonferroni p -value correction. Spearman correlation coefficients (R_s) values highlighted red show a negative correlation, whereas RS values highlighted blue show a positive correlation.

	Shannon	CCC	16S rRNA	Turbidity	Temp	pH	Chl-a	DO	NO ₃ -	TDP
ASV0004_Aphanizomenon	0.24007	0.19907	0.049033	0.39552	0.12614	-0.044474	0.065278	-0.14404	-0.24663	0.17125
ASV0005_Cyanobium	0.1693	0.42775	0.047298	-0.10618	0.1036	-0.35848	-0.63782	-0.63065	-0.016639	0.31506
ASV0006_Planktothrix	0.022895	0.12569	0.21751	0.029515	0.12978	-0.26648	-0.23656	-0.31275	0.10059	0.041804
ASV0007_Synechococcus	0.047988	0.53885	0.17004	0.24482	0.33239	0.25416	-0.0045136	0.065279	-0.20578	-0.18739
ASV0008_Cyanobium	-0.16536	-0.049435	-0.059497	-0.064425	-0.11031	0.46821	0.56957	0.68536	-0.092004	-0.21856
ASV0009_Microcystis	0.21256	0.095783	-0.064783	-0.025959	-0.09784	-0.017674	0.063159	-0.010528	0.078191	-0.031918
ASV0014_Cyanobium	0.37755	0.20849	-0.29517	0.30681	-0.10762	-0.51783	-0.55132	-0.64223	0.30912	0.49326
ASV0016_Snowella	0.37502	0.3778	-0.010639	0.28227	0.21315	-0.11515	-0.23475	-0.38262	-0.0049261	0.10764
Shannon diversity		-0.3262	-0.2148	-0.20678	-0.14929	-0.088712	-0.19854	-0.072275	0.17765	0.2941
CCC	-0.3262		0.24856	0.33644	0.49991	0.09461	-0.07326	-0.24741	-0.36219	-0.15182
16S rRNA-ITS abundance	-0.2148	0.24856		0.085416	0.74694	0.32438	0.32424	0.031744	-0.36927	-0.46901

Table S3 Similarity percentage (SIMPER) test on the cyanobacteria ASVs among the different sample types. Only ASVs with > 1% relative abundance in the sample types were used in the for the test.

Taxon	ASV_ID	Av. sim	Contrib. %	Cumulative %	Mean Water	Mean TrapM	Mean TrapH	Mean Sed
Aphanizomenon sp.	ASV_0004	4.427	9.34	9.34	1.01	3.64	4	5.04
Cyanobium sp.	ASV_0008	3.203	6.758	16.1	2.72	0.852	0.483	0.558
Planktothrix sp.	ASV_0006	2.526	5.328	21.43	2.51	0.586	0.752	0.541
Synechococcus sp.	ASV_0007	2.374	5.008	26.43	3.11	1.98	1.51	1.01
Cyanobium sp.	ASV_0005	2.258	4.765	31.2	2.37	2.02	1.89	1.61
Cyanobium sp.	ASV_0013	2.222	4.689	35.89	2.4	0.865	0.747	0.74
Snowella sp.	ASV_0016	2.219	4.681	40.57	0.906	1.88	2.5	1.02
Cyanobium sp.	ASV_0010	2.151	4.538	45.11	1.77	2.42	2.22	1.9
Cyanobium sp.	ASV_0012	1.969	4.154	49.26	1.42	2.27	1.92	1.65
Cyanobium sp.	ASV_0015	1.948	4.109	53.37	2.12	1.1	0.896	0.68
Cyanobium sp.	ASV_0014	1.898	4.004	57.37	1.4	1.3	2.41	1.12
Cyanobium sp.	ASV_0019	1.83	3.861	61.24	1.77	0.426	0.445	0
Synechococcus sp.	ASV_0021	1.662	3.507	64.74	1.66	0.323	0.456	0.599
Cyanobium sp.	ASV_0031	1.553	3.277	68.02	1.6	0.523	0.499	0
Snowella sp.	ASV_0022	1.553	3.276	71.3	0.786	1.35	1.64	0.476
Cyanobium sp.	ASV_0020	1.446	3.051	74.35	1.09	1.79	1.67	3.99
Aphanizomenon sp.	ASV_0035	1.433	3.024	77.37	0.478	1.29	1.39	2
Cyanobium sp.	ASV_0053	1.314	2.772	80.14	1.07	0.0541	0.0572	0.292
Cyanobium sp.	ASV_0049	1.258	2.653	82.8	0.434	1.12	1.23	0.987
Planktothrix sp.	ASV_0050	1.158	2.443	85.24	0.903	0	0.0651	0
Microcystis sp.	ASV_0009	1.077	2.272	87.51	0.724	0.644	1.02	1.59
Cyanobium sp.	ASV_0030	1.06	2.236	89.75	1.47	0.909	0.78	0.364
Cyanobium sp.	ASV_0028	1.049	2.213	91.96	1.04	0.863	1.26	1.15
Cyanobium sp.	ASV_0056	0.9107	1.921	93.88	0.941	0.236	0.379	0
Cyanobium sp.	ASV_0054	0.8186	1.727	95.61	0.699	0.64	0.811	0.466
Microcystis sp.	ASV_0041	0.7399	1.561	97.17	0.647	0.961	1.03	0.659

Table S4 Total sulphide measurements from water column samples.

Date	Water Depth [m]	Sample ID	Observation	H2S_μmolL-1
30.10.2019	54	54	filtered	2
30.10.2019	55	55a	filtered	7,9
30.10.2019	55	55b	filtered	5,2
30.10.2019	57	57	filtered	33,3
30.10.2019	59,5	59,5	filtered	44,8
30.10.2019	60,8	60,8	filtered	42,5
28.11.2019	53	53	filtered	11
28.11.2019	55	55	filtered	13,7
28.11.2019	57	57	filtered	9,7
28.11.2019	59	59	filtered	34

Table S5 Nitrate measurements from water column samples. NA = not ascertained.

SampleID	NO ₃ ⁻
WMay2_3	0,57
WMay29_3	0,14
WJu27_3	0,19
WAug6_3	NA
WAug28_3	NA
WOc2_3	NA
WOc30_3	NA
WNo28_3	0,30
WJa30_5	2,02
WFe24_5	1,81
WMar28_5	1,40
WMay2_7	1,01
WMay29_7	1,04
WJu27_7	1,52
WAug6_7	NA
WAug28_7	NA
WOc2_7	NA
WOc30_7	NA
WNo28_7	0,19
WMar28_10	1,38
WMay2_10	1,26
WMay29_10	2,51
WJu27_10	1,94
WAug6_10	1,71
WAug28_10	1,08
WOc2_10	0,47

WOc30_10	NA
WNo28_10	0,20
WMay2_15	1,64
WMay29_15	1,85
WJu27_15	2,07
WAug28_15	2,04
WOc2_15	2,31
WOc30_15	2,24
WNov28_15	2,00
WMar28_20	2,16
WAug6_20	2,14
WJa30_45	1,96
WFe24_45	1,74
WMar28_45	1,71
WMay2_45	1,85
WMay29_45	2,02
WJu27_45	1,96
WAug6_45	2,11
WAug28_45	1,73
WOc2_45	2,04
WOc30_45	0,90
WNo28_45	0,75

Table S6

ANOVA test for equal means on species richness from sediments and water column ($P < 0.05$; Figure 4). A subsequent Tukey's pairwise test showed hypolimnion sediment trap cyanobacteria communities to significantly differ to the communities from the epi-, meta and hypolimnion communities of the water column. Tukey's Q below the diagonal and P-values above the diagonal. Significant P-values are in bold. Shapiro Wilk: 0.9915, p_{normal} :0.9447. Where 'W' indicates water column samples from the from the epi-, meta- and hypolimnion, respectively. The 'ST' indicates sediment trap material from the meta- and hypolimnion, respectively. 'Sed' represents the surface sediment samples.

ANOVA Test for equal means across sample types					
	Sum of sqrs	df	Mean square	F	p (same)
Between groups:	1007.74	4	251.935	6,133	0.006964
Within groups:	3279.15	58	64.2957	Permutation p (n=99999)	
Total:	4736.69	62	0.00627		

Tukey's pairwise	W_Epi	W_Meta	W_Hypo	ST_Meta	ST_Hypo
W_Epi		0.9989	0.9982	0.2364	0.03609
W_Meta	0.3772		1	0.2609	0.04405
W_Hypo	0.4292	0.03314		0.1508	0.01942
ST_Meta	2.962	2.884	3.293		0.9518
ST_Hypo	4.165	3.927	4.496	1.014	

Table S7 The significant explanatory parameters used in the Spearman correlation analysis.

Explanatory variable	AIC	Pseudo-<i>F</i>	<i>P</i>
DO	159.73	8.77	0.001
Turbidity	157.26	4.92	0.002
TDP	154.76	4.56	0.002
pH	153.98	4.42	0.005
NO ₃ ⁻	152.98	3.56	0.004
Temperature	150.95	3.07	0.008

The significance of the environmental variables was tested by 999 Monte Carlo permutations and were selected by forward selection (Adjusted $R^2 = 0.34$). AIC = Akaike information criterion.